Inorg. Chem. **2006**, *45*, 7915–7921

The Solution Structures and Dynamics and the Solid-State Structures of Substituted Cyclopentadienyltitanium(IV) Trifluorides

Franc Perdih, Andrej Pevec, Saša Petriček, Andrej Petrič, Nina Lah, Ksenija Kogej, and Alojz Demšar*

Faculty of Chemistry and Chemical Technology, University of Ljubljana, Aškerčeva 5, Ljubljana, Slovenia

Received April 27, 2006

Organotitanium fluorides $(C_5Me_4R)TiF_3$ (R = H, Me, Et) sublimate with formation of crystalline dimers. From solution, we obtained crystals of dimers and tetramers. The tetramer $[\{(C_5Me_5)TiF_3\}_4]$ irreversibly dissociates in the solid state to dimers ($\Delta H = 8.33$ kcal mol^{-1}). The variable-temperature ^{1}H and ^{19}F NMR spectroscopy measurements of the toluene-d_8 solution of $[\{(C_5Me_5)TiF_3\}_2]$ revealed at 202 K one monomeric, two dimeric (with C_{2h} and C_s symmetry), two tetrameric (with D_2 and C_{2v} symmetry), and two trimeric (both C_2 symmetry) molecules. With the increase in temperature and dilution of the solution, the composition of the solution shifts to the smaller molecules. The thermodynamic and activation parameters for the reversible dissociation of dimers to monomers in the solution are $\Delta H = 9.2$ kcal mol^{-1}, $\Delta S = 24.2$ cal mol^{-1} K^{-1}, $\Delta H^{\ddagger} = 12.2$ kcal mol^{-1}, $\Delta S^{\ddagger} = 9.7$ cal mol^{-1} K^{-1}. The dissociation path with a weakly double-bridged transition-state dimer was proposed. The thermodynamic parameters for the reversible dissociation of the C_{2v} tetramer to the dimers in solution are $\Delta H = 7.9$ kcal mol^{-1} and $\Delta S = 26.8$ cal mol^{-1} K^{-1}. From both tetramers, the D_2 molecule is 0.34(5) kcal mol^{-1} lower in enthalpy and 6.5(5) cal mol^{-1} K^{-1} lower in entropy than the C_{2v} molecule. The structures of both trimers were proposed. The low-temperature ^{19}F NMR spectra of the $CDCl_3$ solution of $[\{(C_5Me_5)TiF_3\}_2]$ are consistent with equilibria of a monomer, two dimers (with C_{2h} and C_s symmetry), and a trimer. The vapor pressure osmometric molecular mass determination of $CDCl_3$ solution of $[\{(C_5Me_5)TiF_3\}_2]$ at 302 K is consistent with the equilibrium of the dimer and the monomer.

Introduction

The monomer−dimer−oligomer equilibria in solutions of main group, transition, and lanthanide metal compounds were observed for molecules having both a Lewis-acidic metal atom and a Lewis-basic nitrogen, oxygen, or halogen atom and for organometallic compounds with a metal of pronounced Lewis acidity, such as trimethylaluminum.[1] Particular interest is focused on monomer−dimer−oligomer equilibria of catalysts with a Lewis-acidic metal center.[2] In comparison with the monomer, the Lewis acidity of the metal atoms of the double-bridged dimer is lowered, whereas within the single-bridged dimer, there is a metal atom with increased and another one with decreased Lewis acidity compared with the monomer.[3] Another catalytic behavior, attributed to the formation of the catalyst dimer, is chiral amplification.[2a,b] Chiral amplification is the positive nonlinear relationship between enantiomeric excess (ee) of partially resolved chiral ligand at the metal catalyst and the ee of the reaction product; it is explained on the basis of catalytically active dimers or

* To whom correspondence should be addressed. E-mail: alojz.demsar@fkkt.uni-lj.si.

(1) (a) Santra, B. K.; Liaw, B.-J.; Hung, C.-M.; Liu, C. W.; Wang, J.-C. *Inorg. Chem.* **2003**, *42*, 8866−8871. (b) Bonasia, P. J.; Arnold, J. *Inorg. Chem.* **1992**, *31*, 2508−2514. (c) Kim, G.-S.; DeKock, C. W. *Polyhedron* **2000**, *19*, 1363−1371. (d) Sadique, A. R.; Heeg, M. J.; Winter, C. H. *Inorg. Chem.* **2001**, *40*, 6349−6355. (e) Izod, K.; O'Shaughnessy, P.; Sheffield, J. M.; Clegg, W.; Liddle, S. T. *Inorg. Chem.* **2000**, *39*, 4741−4748. (f) Blair, S.; Izod, K.; Clegg, W. *Inorg. Chem.* **2002**, *41*, 3886−3893. (g) Glas, H.; Kohler, K.; Herdtweck, E.; Maas, P.; Spiegler, M.; Thiel, W. R. *Eur. J. Inorg. Chem.* **2001**, 2075−2080. (h) Entwhistle, C. D.; Marder, T. B.; Howard, J. A. K.; Fox, M. A.; Mason, S. A. *J. Organomet. Chem.* **2003**, *680*, 165−172. (i) Mitzel, N. W.; Lustig, C.; Berger, R. J. F.; Runeberg, N. *Angew. Chem., Int. Ed.* **2002**, *41*, 2519−2522. (j) Berthomieu, D.; Bacquet, Y.; Pedocchi, L.; Goursot, A. *J. Phys. Chem. A* **1998**, *102*, 7821−7827.

(2) (a) Walsh, P. J. *Acc. Chem. Res.* **2003**, *36*, 739−749. (b) Balsells, J.; Davis, T. J.; Carroll, P.; Walsh, P. J. *J. Am. Chem. Soc.* **2002**, *124*, 10336−10348. (c) Terada, M.; Matsumoto, Y.; Nakamura, Y.; Mikami, K. *J. Chem. Soc., Chem. Commun.* **1997**, 281−282. (d) Kitamura, M.; Suga, S.; Oka, H.; Noyori, R. *J. Am. Chem. Soc.* **1998**, *120*, 9800−9809. (e) M.; Suga, S.; Niwa, M.; Noyori, R. *J. Am. Chem. Soc.* **1995**, *117*, 4832−4842. (f) Moore, D. R.; Cheng, M.; Lobkovsky, E. B.; Coates, G. W. *J. Am. Chem. Soc.* **2003**, *125*, 11911−11924.

10.1021/ic060714w CCC: $33.50 © 2006 American Chemical Society
Published on Web 08/15/2006

Chart 1. Schematic Representation of $[\{Cp'TiF_3\}_n]$ Complexes with the Fluorine Atom Labeling Used in the Assignment of ^{19}F NMR Spectra

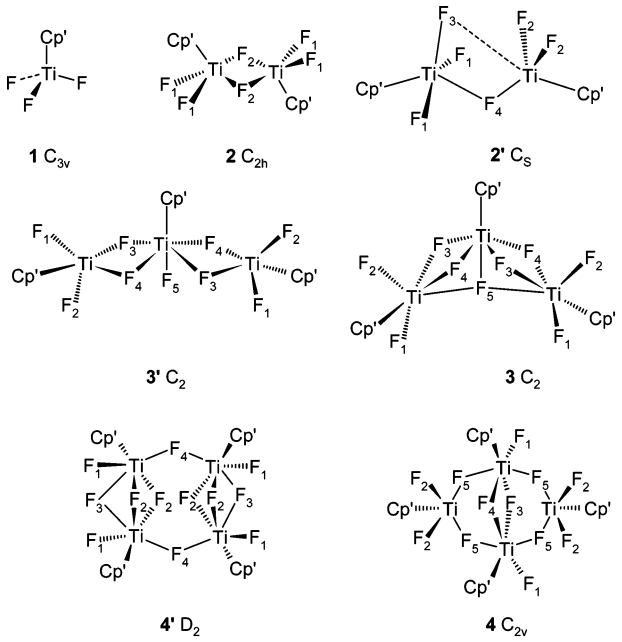

Cp'=C_5Me_5 **a**, C_5Me_4Et **b**, C_5Me_4H **c** (*e.g.* **2a** denotes $[\{C_5Me_5TiF_3\}_2]$)

monomers.[2d] For catalytically active monomers, the thermodynamics of the equilibria of three dimers (R−R, S−S, R−S) and two monomers (R, S) affect the enantioselectivity of the reaction (R and S denotes metallic species with the chiral ligand).[2d]

Homogeneous catalysts formed from metallic fluoride and a chiral ligand offer unique catalytic properties due to the high electronegativity of fluorine[4] and bifunctional catalysis with the interaction of fluorine atom with fluorophilic atoms of reagents such as silicon and aluminum.[5] The chiral amplification observed for the enantioselective addition of allyltrimethylsilane and trimethylaluminum to aldehydes was explained with active catalyst monomer species $[(L)TiF_2]$ (L = BINOLate, TADDOLate).[6] This suggests that a monomer−dimer equilibrium of fluorometallic species likely exists in this system. We found that organotitanium trifluorides $(C_5Me_4R)TiF_3$ (R = H, Me, Et)[7] are suitable for studying the thermodynamics and kinetics of the dimerization and oligomerization equilibria that could be relevant for

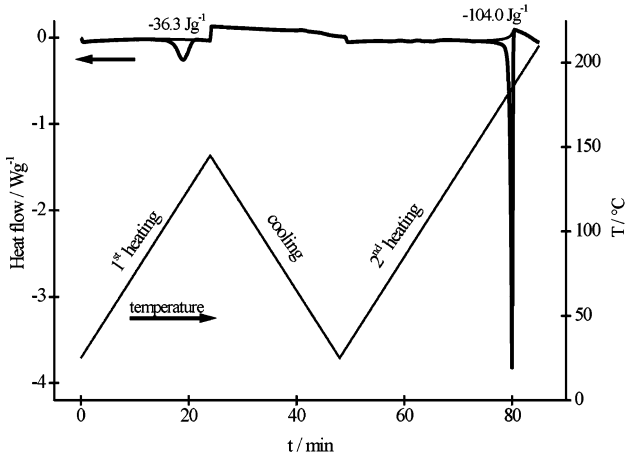

Figure 1. DSC curve of **4a**.

equilibria of fluorometallic catalyst species and could help in the understanding and development of homogeneous fluorometallic catalytic systems. The monomer, two dimers, two trimers, and two tetramers and their equilibria were observed in a solution of $(C_5Me_4R)TiF_3$. The tools used in the present study are variable-temperature ^1H and ^{19}F NMR spectroscopy, vapor pressure osmometry, IR spectroscopy of solutions, and for crystallized substances, DSC and X-ray structure determination.

Results

Solid State: X-ray Structures and Thermal Analysis. The structures of the species appearing in this report are shown in Chart 1. The X-ray structures of crystals obtained from solutions previously[7a,8] and in this work (see the Supporting Information for structures of tetrameric **4a** and **4c**) revealed dimeric (**2**) and tetrameric (**4**) molecules. The formation of crystalline tetramers is favored by a low temperature of crystallization and high solubility of $(C_5Me_4R)TiF_3$. This behavior can be explained by the equilibrium of the dimers and the tetramers observed in a solution of $(C_5Me_5)TiF_3$ by ^{19}F and ^1H NMR spectroscopy (see below). The crystals of the sublimated $(C_5Me_4R)TiF_3$ are built from dimeric molecules, according to X-ray structure determinations (see the Supporting Information for structures of dimeric **2a** and **2b**).

The curve obtained by dynamic scanning calorimetry (DSC) of **4a** is shown in Figure 1. A broad endothermic transition occurs between 90 and 130 °C during the first heating to 145 °C. The transition is irreversible, because an exothermic transition was not observed at cooling of the sample to 25 °C. During the second heating cycle to 230 °C, a sharp endothermic transition appeared at 180 °C. A transition at the same temperature was observed in the DSC curve of **2a** (not shown) and is in agreement with the melting point of **2a**.[7a] The irreversible transition between 90 and 130 °C could be attributed to the dissociation of tetrameric **4a** to dimeric **2a** in the solid state with $\Delta H = 8.3$ kcal mol^{-1} (calculated per mol of **4a**). The enthalpy of melting $\Delta H_{fus} = 11.8$ kcal mol^{-1} (calculated per mol of **2a**).

(3) (a) Negishi, E. *Chem.—Eur. J.* **1999**, *5*, 411−420. (b) Negishi, E. *Dalton Trans.* **2005**, 827−848.
(4) (a) Murphy, E. F.; Murugavel, R.; Roesky, H. W. *Chem. Rev.* **1997**, *97*, 3425−3468. (b) Pagenkopf, B. L.; Carreira, E. M. *Chem.—Eur. J.* **1999**, *5*, 3437−3442. (c) Mezzetti, A.; Becker, C. *Helv. Chim. Acta* **2002**, *85*, 2686−2703. (d) Fagnou, K.; Lautens, M. *Angew. Chem., Int. Ed.* **2002**, *41*, 26−47.
(5) (a) Duthaler, R. O.; Hafner, A. *Angew. Chem., Int. Ed.* **1997**, *36*, 43−45. (b) Shibasaki, M.; Kanai, M.; Funabashi K. *Chem. Commun.* **2002**, 1989−1999. (c) Denmark, S. E.; Fu, J. *Chem. Rev.* **2003**, *103*, 2763−2794.
(6) (a) Gauthier, D. R., Jr.; Carreira, E. M. *Angew. Chem., Int. Ed.* **1996**, *35*, 2363−2365. (b) Bode, J. W.; Gauthier, D. R., Jr.; Carreira, E. M. *Chem. Commun.* **2001**, 2560−2561. (c) Pagenkopf, B. L.; Carreira, E. M. *Tetrahedron Lett.* **1998**, *39*, 9593−9596.
(7) (a) Sotoodeh, M.; Leichtweis, I.; Roesky, H. W.; Noltemeyer, M.; Schmidt, H.-G. *Chem. Ber.* **1993**, *126*, 913−919. (b) Herzog, A.; Liu, F.-Q.; Roesky, H. W.; Demsar, A.; Keller, K.; Noltemeyer, M.; Pauer, F. *Organometallics* **1994**, *13*, 1251−1256.
(8) Kunzel, A.; Parisini, E.; Roesky, H. W.; Sheldrick, G. M. *J. Organomet. Chem.* **1997**, *536*, 177−180.

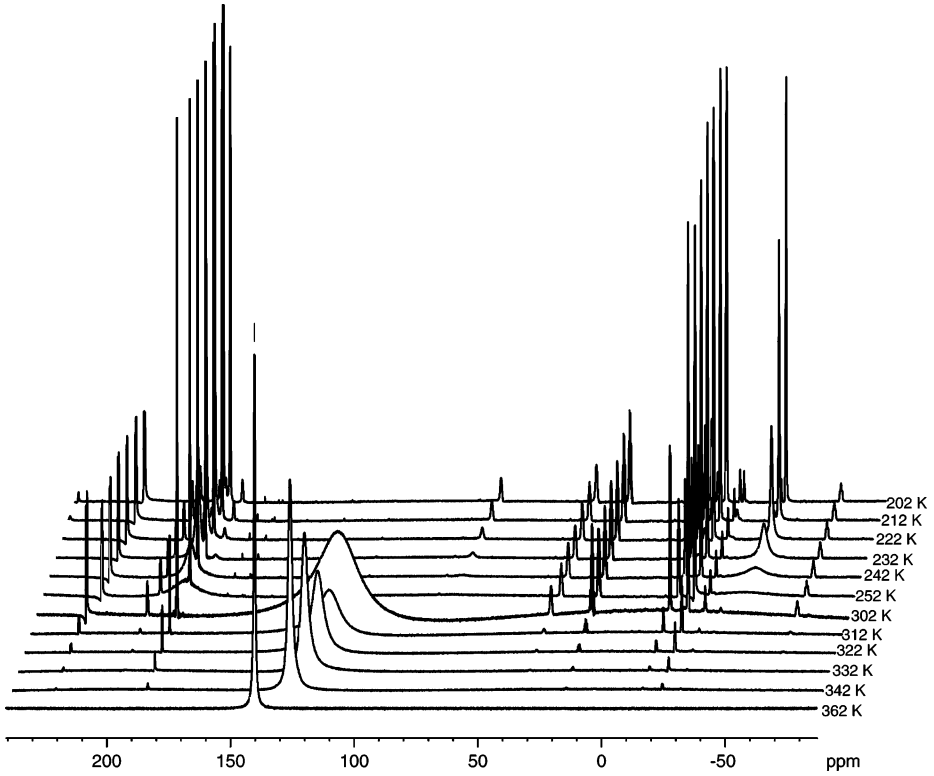

Figure 2. VT ^{19}F NMR spectra of a 0.19 M toluene-d_8 **2a** solution.

Solution Molecular Weight Determination. The average molecular mass of solute, determined by the vapor pressure osmometry of 0.026 M **2a** solution in $CHCl_3$ at 302 K, is $3.4(1)\cdot10^2$ g mol^{-1}. The ^{19}F NMR spectrum of $CDCl_3$ solution of **2a** at 302 K displays only a broad resonance suggesting equilibrium of **1a** and **2a**. Assuming this equilibrium, the average molecular mass corresponds to 40(2)% dimer **2a** dissociated to monomer **1a** in this solution.

Variable-Temperature (VT) ^{1}H and ^{19}F NMR Spectroscopy. (i) Solution of 2a in Toluene-d_8. The variable-temperature ^{19}F NMR spectra of a 0.19 M toluene solution of **2a** are presented in Figure 2 and Table S6 of the Supporting Information. The low-temperature (202 K) ^{19}F NMR spectrum of **2a** is assigned in Table 1. The species observed by ^{1}H and ^{19}F NMR in a 0.19 M toluene solution and in a 0.08 M $CDCl_3$ solution of **2a** are shown in Chart 1. Thermodynamic and activation parameters of processes studied are in Table 2. A single broad ^{19}F NMR resonance of **2a** and **2b** observed at room temperature[7] unearths, at a higher concentration of solution (0.19 M) and variation in the temperature, a variety of equilibrating species. The low-temperature (202 K) ^{19}F NMR spectrum (Table 1, and Figure S4 of the Supporting Information) of **2a** toluene-d_8 (0.19 M) solution shows resonances of **2a** (two, C_{2h}), **3a** (five, C_2), **3′a** (five, C_2), **4a** (five, C_{2v}) and **4′a** (four, D_2) in concentration ratio 1(**2a**):0.14(**3a**):0.08(**3′a**):0.62(**4a**):0.092-(**4′a**). The assignment of the resonances was done on the basis of chemical shifts of fluorine resonances observed in cyclopentadienyltitanium fluorides.[9,10] The resonances of species **2a** and **4a** are in agreement with their structures in the solid state, suggesting that their structures observed in the solid-state are retained in the solution. The structure of **4′a** is proposed on the basis of the structural motif found in

Table 1. Assignment of the Resonances in the ^{19}F NMR Spectrum of **2a** Solution[a]

δ (ppm)[b]	molecule[c]	atom[c]	relative intensity
239.25 m	3′a	F5	0.04
212.68 m	4a	F1	0.63
190.09 s	4′a	F1	0.18
183.81 s	3a	F1	0.15
182.20 s	3′a	F1 or F2	0.09
180.80 m	2a	F1	2.04
179.75 s	3′a	F1 or F2	0.07
177.90 m	4a	F2	1.22
173.17 s	3a	F2	0.14
68.50 m	3a	F3	0.14
29.85 m	4′a	F2	0.20
16.27 m	4a	F3	0.31
−16.78 m	4a	F4	0.30
−19.37 m	3a	F4	0.13
−22.78 m	4a	F5	1.27
−28.27 m	4′a	F3	0.10
−29.92 m	3′a	F3	0.08
−44.81 m	3′a	F4	0.08
−45.86 m	2a	F2	1.00
−69.17 m	4′a	F4	0.08
−104.65 m	3a	F5	0.07

[a] Toluene-d_8 (0.19 M) solution at 202 K. [b] s singlet, m multiplet. [c] see Chart 1.

(9) Pevec, A.; Demšar, A.; Gramlich, V.; Petriček, S.; Roesky, H. W. *J. Chem. Soc., Dalton Trans.* **1997**, 2215−2216.

(10) (a) Perdih, F.; Demšar, A.; Pevec, A.; Petriček, S.; Leban, I.; Giester, G.; Sieler, J.; Roesky, H. W. *Polyhedron* **2001**, *20*, 1967−1971. (b) Demsar, A.; Pevec, A.; Petriček, S.; Golič, L.; Petrič, A.; Bjorgvinsson, M.; Roesky, H. W. *J. Chem. Soc., Dalton Trans.* **1998**, 4043−4047. (c) Demšar, A.; Pevec, A.; Golič, L.; Petriček, S.; Petrič, A.; Roesky, H. W. *Chem. Commun.* **1998**, 1029−1030. (d) Pevec, A.; Perdih, F.; Košmrlj, J.; Modec, B.; Roesky, H. W.; Demšar, A. *Dalton Trans.* **2003**, 420−425.

Table 2. Enthalpy and Entropy Changes for Reversible Reactions in a Toluene-d_8 Solution of **2a** and for DSC Measurements in the Solid State[a]

reaction	ΔH	ΔS	method
2a(solv) ↔ 2 **1a**(solv)	9.2	24.2	VT ^{19}F NMR in fast exchange
2a(solv)↔ 2 **1a**(solv)	12.2[b]	9.7 [c]	VT ^{19}F NMR line shape analysis
2a(s) ↔ **2a**(l)	11.8		DSC
4a(solv)↔ 2 **2a**(solv)	7.9	26.8	VT ^{1}H NMR in slow exchange
4a(s) → 2 **2a**(s)	8.3		DSC
4a(solv) ↔ **4′a**(solv)	−0.34(5)	−6.5(5)	VT ^{19}F NMR in slow exchange

[a] ΔH in kcal mol^{-1}, ΔS in cal mol^{-1} K^{-1}. [b] Activation enthalpy ($\Delta H^{\ddagger}$). [c] Activation entropy ($\Delta S^{\ddagger}$)

the solid-state structures of [{(C_5Me_5)MF_3}$_4$] (M = Zr, Hf).[7b] The dilution of a **2a** toluene-d_8 solution from 0.19 to 0.02 M (at 202 K) changes the concentration ratio to 1(**2a**):0.06(**3a**):0.04(**3′a**):0.14(**4a**):0.03(**4′a**). However, the equilibrium constants K_{2a-3a}, K_{2a-4a}, and $K_{2a-4'a}$ (see eqs 1−5 for equilibrium constants) are similar for 0.19 and 0.02 M solutions. This finding supports the proposed nuclearity of dimers, trimers, and tetramers.

$$K_{1a-2a} = (C_{2a})/(C_{1a})^2 \quad (1)$$

$$K_{2a-3a} = (C_{3a})^2/(C_{2a})^3 \quad (2)$$

$$K_{2a-4a} = (C_{4a})/(C_{2a})^2 \quad (3)$$

$$K_{2a-4'a} = (C_{4'a})/(C_{2a})^2 \quad (4)$$

$$K_{4a-4'a} = (C_{4'a})/(C_{4a}) = K_{2a-4'a}/K_{2a-4a} \quad (5)$$

The variable-temperature ^{19}F NMR spectra of a 0.19 M toluene solution of **2a** (Figure 2 and Table S6 of the Supporting Information) display changes in the resonances of the dimer, both trimers, and both tetramers. Two **2a** resonances, with an increase in temperature, first lose the multiplet structure at 212 K and then broaden and disappear in the baseline at 272 K; a single broad resonance appears above 302 K. This single resonance sharpens; its chemical shift increases with the increase in temperature and at dilution of solution (Figure S5 of the Supporting Information). The ^{19}F NMR resonances of **3a** and **3′a** are multiplets at 202 K that broaden and disappear in the baseline at 242 and 222 K, respectively. The resonances of both tetramers diminish with the increase in temperature and disappear without the line broadening at 342 (**4′a**) and 362 K (**4a**).

Three mechanisms that can participate in the coalescence of two **2a** resonances to the single resonance have been considered (Scheme 1): (1) equilibrium of dimeric **2a** and monomeric **1a**, (2) the exchange of terminal and bridging fluorine atoms by a single-bridged intermediate, and (3) the exchange of terminal and bridging fluorine atoms by a triple-bridged intermediate. The observation that the dilution of the **2a** solution causes the shift of the ^{19}F and ^{1}H NMR resonance (Figure S5 of the Supporting Information) suggests an intermolecular mechanism for the coalescence of the fluorine resonance. The observed changes in the spectra are in agreement with the equilibrium of dimer **2a** and monomer **1a** proposed in Scheme 1. This equilibrium should be shifted to monomeric **1a** with the increase in temperature and dilution of the solution. However, simultaneously running intramolecular mechanisms with single- or triple-bridged intermediates (Scheme 1) cannot be ruled out.

Scheme 1

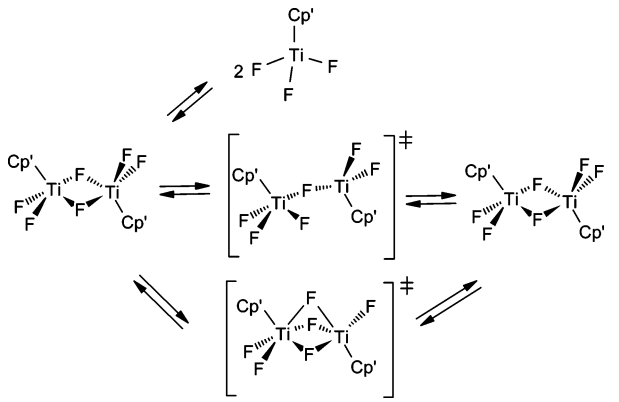

The structures of trimers **3a** and **3′a** (Chart 1) with C_2 symmetry were proposed solely on the basis of their ^{19}F NMR spectra. The formation of **3′a** from **2a** and **1a** could be proposed by formation of a (μ-F)$_2$ bridge from two terminal fluorine atoms and resembles dimerization of **1a** to **2a**. The trimers are likely stable intermediate species in the formation of tetramers **4a** and **4′a** from the dimers. The broadening of the ^{19}F NMR resonances **3a** and **3′a** could be explained by their dissociation to dimer **2a** and to the monomer and also by the interconversion of **3a** and **3′a**. The proposed structures of **3′a** and **3a** allow facile wing-moving interconversion between both trimeric molecules. The bending of **3′a** results in coordination of the central terminal fluorine atom to another two titanium atoms and the formation of **3a**.

The ^{19}F NMR resonances of both tetramers in the variable-temperature spectra show an increase in the ratio **4a**/**4′a** with increasing temperature, from 5.4 at 212 K to 7.5 at 312 K. The values of $K_{4'a-4a}$ fit the ln($K_{4'a-4a}$) versus 1/T plot (R^2 = 0.99) in the temperature range from 262 to 302 K. The thermodynamic parameters for the equilibrium of tetramers show that the conversion of **4a** to **4′a** is slightly exothermal (−0.34(5) kcal mol^{-1}) with a decrease in entropy (−6.5(5) cal mol^{-1} K^{-1}). The direct intramolecular conversion of **4a** to **4′a** seems unlikely. The interconversion between **4a** and **4′a** is probably achieved by the equilibria of dimer, trimers, and tetramers. The equilibrium of both tetramers **4a** and **4′a** is observed in the solution of titanium compound **2a** and only a single tetramer with the structural motif of **4′a** is found in the solution of [{Cp*MF_3}$_4$] (M = Zr, Hf).[7b]

The VT ^{1}H NMR spectra of a **2a** toluene-d_8 (0.19 M) solution show methyl-ring resonances of **4′a** (one) and **4a** (two) and a single resonance of **2a** and **1a** in fast exchange (Figure S6 of the Supporting Information). The changes in VT ^{1}H NMR spectra are in agreement with the processes proposed from the VT ^{19}F NMR spectra.

The plots of observed chemical shifts of the **2a**/**1a** ^{19}F NMR resonance in fast exchange versus concentration were used for calculations of dimerization constants (K_{1a-2a}) in the temperature range 312−362 K (Figure S7 of the Supporting Information). The chemical shifts of the reso-

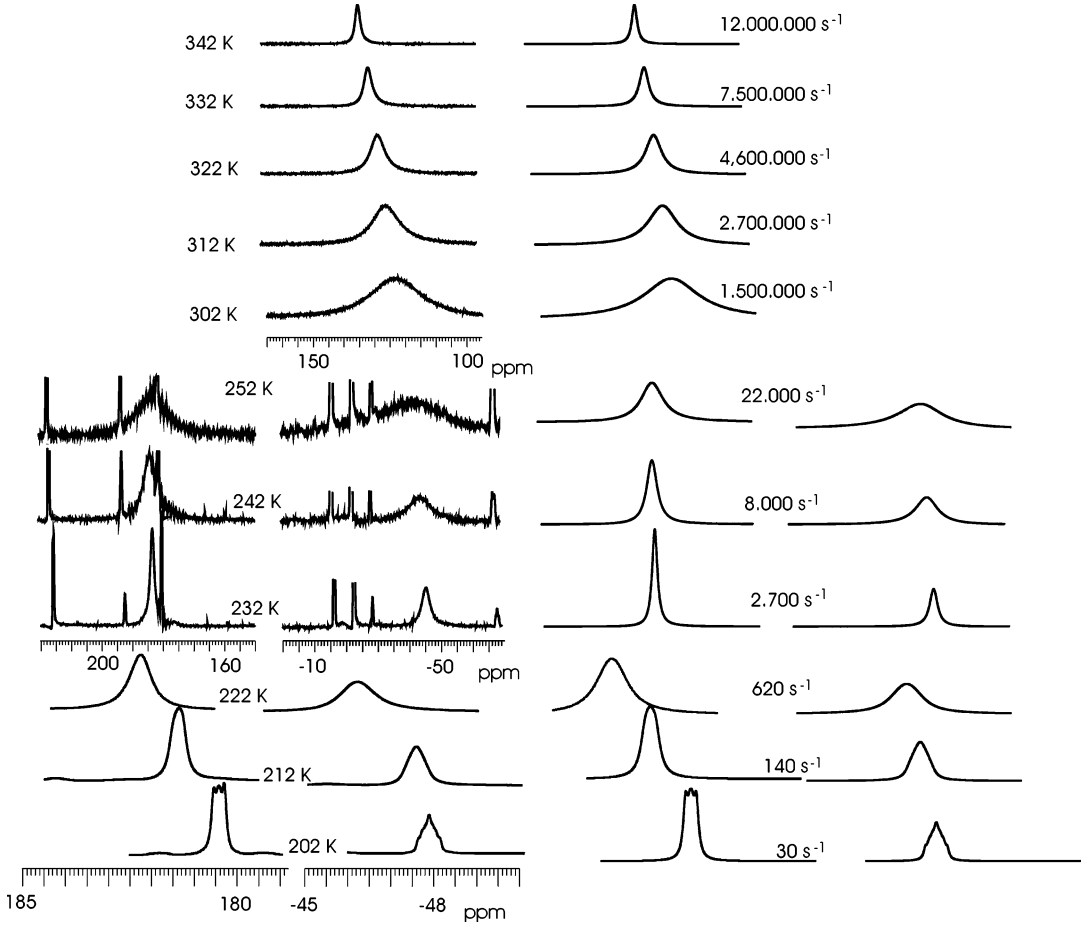

Figure 3. Observed (left) and calculated (right) ^{19}F NMR resonances of **2a** (202−252 K) and **2a**/**1a** (302−342 K). Rate constants are for the dissociation of **2a**.

nance in the fast-exchange regime of the 2**1a** ↔ **2a** equilibrium depend on the dimerization constant, chemical shifts of **1a** (δ_{1a}) and **2a** (δ_{2a}), and concentration as expressed by eq 6.[11]

$$\delta_{obs} = \delta_{1a} + \frac{1 + K_{1a-2a}C - \sqrt{1 + 8K_{1a-2a}C}}{4K_{1a-2a}C}(\delta_{2a} - \delta_{1a}) \quad (6)$$

where C is titanium concentration in solution in the form of monomers **1a** and dimers **2a**, $C = 2C_0 - 4C_{4a} - 4C_{4'a}$, and C_0 is the formal concentration of **2a** calculated from the amount of **2a** dissolved. The chemical shift of **2a** (δ_{2a}) is the intensity-averaged value of both **2a** resonances and shows temperature dependency in the slow-exchange regime. Using the nonlinear curve-fitting procedure, we calculated the dimerization constant (K_{1a-2a}) and chemical shift of **1a** (δ_{1a}) for each temperature. The ln K_{1a-2a} versus $1/T$ plot (Figure S8 of the Supporting Information) resulted in thermodynamic parameters for the dimerization $\Delta H_{1a-2a} = -9.2 \pm 0.7$ kcal mol^{-1} and $\Delta S_{1a-2a} = -24.2 \pm 3$ cal mol^{-1} K^{-1}. The calculation with the determinated ΔH_{1a-2a} and ΔS_{1a-2a} at 302 K for a 0.026 M solution of dimer **2a** results in 47% **2a** dissociated to monomer **1a**. For comparison, 40% dissociated dimer was obtained for a $CHCl_3$ solution of the same concentration and temperature with the vapor pressure osmometric molecular mass determination.

The full line-shape analysis[12] of fluorine resonances of **2a** was used for the determination of dissociation rate constants for the equilibrium **2a** ↔ 2**1a** (Scheme 1a). The observed and simulated resonances from 202 to 342 K are shown in Figure 3, the corresponding Eyring plot (Figure S9 of the Supporting Information) results in dissociation activation parameters $\Delta H^{\ddagger} = 12.2$ kcal mol^{-1} and $\Delta S^{\ddagger} = 9.7$ cal mol^{-1} K^{-1}.

(ii) VT ^{19}F NMR Spectroscopy of 2a and 2c in $CDCl_3$. The ^{19}F NMR spectrum of a 0.08 M $CDCl_3$ solution of **2a** at 232 K (Figure S10 of the Supporting Information) shows resonances of **2a**, **3a**, and four resonances of an additional minor species in a 2:2:1:1 intensity ratio, tentatively assigned to dimer **2′a** (Chart 1) with C_S symmetry. The proposed structure of dimer **2′a** has a single-bridging fluorine atom (F_4), whereas the ^{19}F NMR resonance of the terminal F_3 atom (103.4 ppm) suggests weak bridging interaction. The molecule **2′a** is polar and its presence in $CDCl_3$ solvent could be due to the stabilization by solvation with the polar $CDCl_3$ solvent. The resonances of tetrameric **4a** and **4′a** were not observed in **2a** deuteriochloroform solution in contrast to the **2a** toluene-d_8 solution. Similarly, as in the toluene-d_8

(11) Schmuck, C.; Wienand, W. *J. Am. Chem. Soc.* **2003**, *125*, 452−459.

(12) Budzelaar, P. H. M. *gNMR*, version V 5.0; Ivorysoft: Oxford, U.K., 2002.

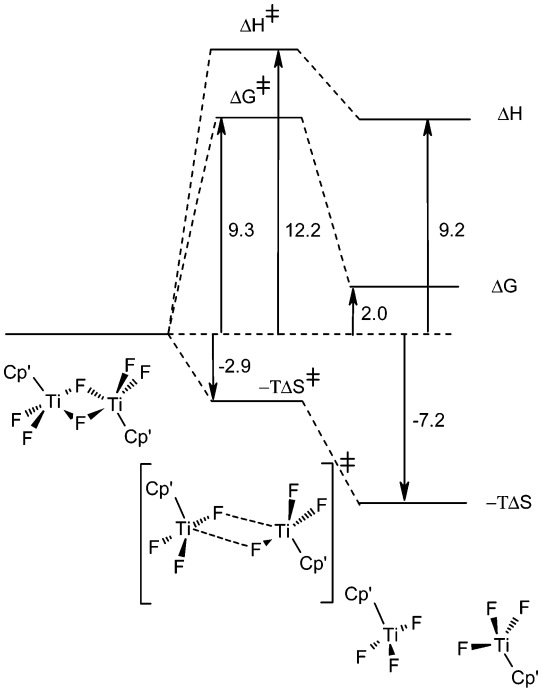

Figure 4. Thermodynamic and activation parameters (kcal mol^{-1}) for the dissociation of **2a** at 298.15 K in toluene-d_8.

solution, two **2a** resonances broaden and disappear in the baseline at 272 K upon an increase in temperature, and a single broad resonance appears above 302 K. The resonances of **3a** and of **2′a** broaden and disappear in the baseline at 262 and 272 K, respectively. Interestingly, the five resonances in a 2:2:2:2:1 intensity ratio, ascribed to trimeric **3c**, were observed as a single species below 252 K in a $CDCl_3$ solution of $(C_5Me_4H)TiF_3$ (see Figure S10 of the Supporting Information and the Experimental Section). We were unable to obtain crystals that were suitable for X-ray structure determination from chloroform solution of $(C_5Me_4H)TiF_3$ at low temperature to confirm the proposed structure of **3c**.

(iii) Discussion of the Mechanisms of the Interconversions. Using the activation and thermodynamic parameters for dissociation of **2a** in toluene (Figure 4) the dissociation mechanism was proposed. Two transition states were considered: (1) the dimer with a single fluorine bridge and another weak bridging interaction with the **2′a** structure (Chart 1), and (2) a double-bridged dimer with two weak bridging interactions or weak association of two dimers (Figure 4). From Figure 4, we can establish the cause of the activation free energy barrier during the dissociation path. The formation of the transition state consumes energy ($\Delta H^{\ddagger}$), but most of the entropy gain ($-T\Delta S$) is released just on the path from the transition state to the separated monomers. The described path is consistent with the proposed mechanism with two weak interactions in the transition state. In addition, the formation of polar transition state **2′a** seems less likely because of the nonpolar toluene-d_8 medium. For the prediction of the dissociation mechanism of **2a** in a toluene-d_8 solution, we can also use the results of the theoretical calculations for dimerization-dissociation reactions between tetrahedral TiF_4 and Ti_2F_8 (C_{2h}, asymmetric $(\mu\text{-F})_2$ bridge).[13] The dissociation of Ti_2F_8 is endothermic with an energy of 10.5 kcal mol^{-1} at the MP2/TZVP(g) level. The energies of Ti_2F_8 (C_{2h}) species with increasing Ti···Ti distance (gradual elongation of two Ti−F bridging bonds with a weakly bonded dimeric transition state and transformation to tetrahedral TiF_4) were calculated to simulate the dissociation; they revealed a barrierless dimerization process in the gas phase.[13] The activation enthalpy for dissociation of **2a** is 12.2 kcal mol^{-1} (Figure 4), and the enthalpy barrier for the dimerization of **1a** is 3.0 kcal mol^{-1}. We can suppose that the enthalpy barrier for dimerization is mainly due to desolvation of monomers **1a** and that the dimerization of two isolated **1a** molecules would be a process with a small enthalpy barrier or without the barrier.

IR Solid State and Solution Spectra. The solid-state IR spectra (Nujol mull) in the 900−400 cm^{-1} range of dimer **2a** and tetramer **4a** show Ti−F stretching of terminal fluorines (**2a**: 638 and 613 cm^{-1}; **4a**: 635, 620, and 583 cm^{-1}) and bridging fluorines (**2a**: 476 cm^{-1}; **4a**: 483 cm^{-1} (Figure S11 of the Supporting Information). The bands of sublimated $C_5Me_5HTiF_3$ at 609 and 640 cm^{-1} also indicate its dimeric structure. The IR spectrum of a benzene solution of **2a** (0.1 M) shows weak 613 and 476 cm^{-1} bands of **2a** and an additional strong band at 806 cm^{-1}. For the pianostool monomer **1a**, two stretching and three deformation IR active vibrations of TiF_3 moiety are expected.[14] Two stretching vibrations should appear at frequencies similar to ν_1 and ν_3 vibration modes of tetrahedral TiF_4 (712 and 793 cm^{-1}).[15] The 806 cm^{-1} band of benzene **2a** solution is therefore assigned to the one of both Ti−F stretching modes of monomeric $[(C_5Me_5)TiF_3]$ **1a**. A higher concentration of solution was achieved using more-soluble **2b** (1.0 M). The IR spectrum of this benzene solution shows strong absorption bands of **2b** (640 and 612 cm^{-1}) and **1b** (803 cm^{-1}), whereas the band with 580 cm^{-1} suggests the presence of **4b** (Figure S11d of the Supporting Information). The solution IR spectra are consistent with the equilibrium of dimer and monomer in a 0.1 M solution, whereas in a 1.0 M solution, the dimer/monomer concentration ratio increases, and tetramer is also observed.

Conclusion

The ^{1}H and ^{19}F NMR spectra revealed equilibria of seven different species in the solutions of $(C_5Me_4R)TiF_3$ (R = H, Me, Et) ranging from monomer to tetramer. The thermodynamics and kinetics of dimerization and dissociation involving monomers and dimers allowed for the prediction of the mechanisms of these processes. It is obvious that the relative stabilities of dimers and monomers of species with a Ti−F bond depend on the other groups bonded to titanium. However, the equilibrium of **1a** and **2a** suggests that both monomer and Ti−$(\mu$-F$)_2$−Ti dimer can be expected for

(13) Webb, S. P.; Gordon, M. S. *J. Am. Chem. Soc.* **1999**, *121*, 2552−2560.
(14) Bencze, É.; Mink, J.; Németh, C.; Herrmann, W. A.; Lokshin, B. V.; Kühn, F. E. *J. Organomet. Chem.* **2002**, *642*, 246−258.
(15) Nakamoto, K. *Infrared and Raman Spectra of Inorganic and Coordination Compounds: Theory and Applications in Inorganic Chemistry*, 5th ed.; Wiley-Interscience: New York, 1997; Vol. A, p 189.

compounds with a Ti−F bond. The equilibrium constant K_{1a-2a} for dimerization of **1a** to **2a** is 29 M^{-1} at 298 K, resulting in comparable concentrations of both species; for example, one-half of the dissolved dimer is dissociated to monomers in a 0.017 M toluene-d_8 solution at 298 K. This equilibrium could help in understanding the behavior of the homogeneous fluorotitanium catalysts[5,6] and suggests catalysis with the more-active monomers, as already proposed.[5a] The catalytic system with a dimerization constant comparable to K_{1a-2a} and with partially resolved chiral ligands on titanium could achieve the chiral amplification on the basis of the catalytically active monomers.[2d] The additional requirements for the chiral amplification in such a system are different stabilities of the homochiral and heterochiral dimer.

Experimental Section

General Considerations. All experimental manipulations were carried out under a nitrogen or argon atmosphere using standard Schlenk techniques or a drybox. Solvents were dried over a Na/K alloy and distilled prior to use. Deuterated NMR solvents were treated with CaH_2, distilled, and stored under argon. DSC measurements were performed on a Mettler Toledo DSC 822^e cell. The sample was weighed in a 40 μL aluminum pan and then hermetically sealed. The empty pan served as a reference. For measurements, the following temperature program was used: from 25 to 145 °C, the furnace was heated at 5 K min^{-1}, cooled with the same rate, and then heated again to 210 °C at 5 K min^{-1}. Vapor-pressure measurements were made with a Knauer vapor-pressure osmometer standardized with a chloroform solution of benzyl alcohol.

NMR spectra were recorded on a Bruker DPX 300 spectrometer operating at 300 (^{1}H) and 282 MHz (^{19}F). The spectra are referenced to Me_4Si and $CFCl_3$ (external standard). Infrared spectra (Nujol mull or benzene solution) were recorded on a Perkin−Elmer FT-1720X spectrometer. $(C_5Me_4R)TiF_3$ (R = Me, Et), Me_3SnF, and $(C_5Me_4H)TiCl_3$ were prepared according to the literature.[7b,16,17]

Synthesis of $(C_5Me_4H)TiF_3$. In a Schlenk flask, $(C_5Me_4H)TiCl_3$ (551 mg, 2 mmol), Me_3SnF (551 mg, 6 mmol), and toluene (50 mL) were stirred for 24 h at room temperature. The resulting solution was filtered to remove the traces of unreacted Me_3SnF, and the filtrate was evaporated to dryness. The solid residual was sublimated at 120 °C, resulting in an orange-red sublimate (260 mg, 58%). Mp: 173 °C. Anal. Calcd for $C_9H_{13}F_3Ti$: C, 47.82; H, 5.80. Found: C, 47.02; H, 6.36. IR (Nujol mull): 1026, 862, 801, 640, 609, 480 cm^{-1}. ^{1}H NMR ($CDCl_3$): δ 2.11 (s, 6 H, 2 × CH_3), 2.19 (s, 6 H, 2 × CH_3), 6.07 (s, 1 H, C_5Me_4H). ^{19}F NMR ($CDCl_3$, 302 K): δ 124 ($w_{1/2}$ = 11000 Hz). ^{19}F NMR ($CDCl_3$, 222 K): δ 160.6 (s, 2 F), 148.6 (s, 2 F), 55.3 (s, 2 F), −23.9 (s, 2 F), −103.0 (s, 1 F).

Variable-Temperature NMR Analysis. The solutions for variable-temperature ^{1}H and ^{19}F NMR studies were prepared in a dinitrogen-filled drybox. The samples were kept for 12 min at the selected temperature before we recorded the spectra. The recorded spectra were processed with 1D WIN NMR and imported into gNMR1.[12] The ^{19}F NMR spectrum of a **2a** toluene solution at 202 K was used for simulation of both resonances of **2a** (see Figure S12 of the Supporting Information for observed and calculated resonances and coupling constants). The dissociation rate constant 30 s^{-1} was included in this simulation. The temperature dependency of the averaged ^{19}F NMR chemical shift was observed for **4a** and **4′a**. The averaged chemical shifts of **4a** and **4′a** satisfactorily fit the quadratic equation in the temperature range 222−332 K (Figure S13 of the Supporting Information). On this basis, the averaged chemical shift (used for calculation of K_{1a-2a}) of both resonances of **2a** (δ_{2a}) in the fast-exchange temperature range 312−362 K were extrapolated from the chemical shifts of **2a** in the slow-exchange regime[18] (Figure S13 of the Supporting Information). Both fluorine resonances of **2a** in the temperature range 202−252 K and the single resonance between 302 and 362 K were used for the determination of dissociation rate constants for the equilibrium **2a** ↔ 2**1a** using full line-shape analysis.[12] The concentrations of **1a** and **2a** used in the simulation were calculated from the corresponding K_{1a-2a} values. The dissociation first-order rate constants were precalculated with a simplified exchange system of two terminal and one bridging fluorine atom of **2a** and three fluorine atoms of **1a**. An iterative full line-shape analysis of the exchange of the full system of six fluorine atoms of **2a** and six fluorine atoms of **1a** was then performed. Two ^{19}F NMR resonances of **2a** were observed below 272 K in slow exchange, whereas the resonance of **1a** was not observed. The simulation of the resonance of **1a** with the determinated thermodynamic and activation parameters in the slow-exchange regime revealed a short lifetime and low concentration of **1a** that results in an unobservable broad and low-intensity resonance. The equilibria involving tetramers (eqs 3−5) were evaluated above 262 K because below this temperature, the ln K vs $1/T$ plots show a declination from linearity. Below 262 K, the equilibrium reactions involving tetramers are likely too slow to fully reach the equilibrium concentrations during the 12 min temperature adjustment.

Acknowledgment. On the occasion of the 70th birthday of Professor Herbert W. Roesky, we dedicate to him this work on the compounds first prepared in his laboratory. This work was supported by Grant PS-0175 from the Ministry of Higher Education, Science and Technology, Republic of Slovenia. Thanks are given to Dr. Romana Cerc-Korošec for DSC measurements.

Supporting Information Available: Data (including X-ray crystallographic files in CIF format) and plots for X-ray structure determination of sublimated **2a**, sublimated **2b**, **4a**, and **4c**·2Me_3SnCl; NMR and IR data, plots, and analysis. This material is available free of charge via the Internet at http://pubs.acs.org.

IC060714W

(16) Zhang, Y.; Mu, Y. *Organometallics* **2006**, *25*, 631−634.
(17) Vela, J.; Smith, J. M.; Yu, Y.; Ketterer, N. A.; Flaschenriem, C. J.; Lachicotte, R. J.; Holland, P. L. *J. Am. Chem. Soc.* **2005**, *127*, 7857−7870.
(18) Reich, H. J. In *WinDNMR: Dynamic NMR Spectra for Windows*; J. Chem. Educ. Software; Division of Chemical Education, American Chemical Society: Washington, D.C., 1996; Vol. 3D, No. 2.